UNIVERSIDAD SAN FRANCISCO DE QUITO USFQ

Colegio de Ciencias e Ingeniería

Characterization of the structural color of a Canthon fulgidus specimen

María José Villamarín Urquizo

Física

Trabajo de titulación presentado como requisito

para la obtención del título de

Físico

Quito, 14 de Mayo de 2023

UNIVERSIDAD SAN FRANCISCO DE QUITO USFQ

Colegio de Ciencias e Ingeniería

HOJA DE CALIFICACIÓN DE TRABAJO DE FIN DE CARRERA

Characterization of the structural color
of a Canthon fulgidus specimen

María José Villamarín Urquizo

Nombre del profesor, Título académico: Melissa Infusino, PhD

Quito, 14 de Mayo de 2023

© Derechos de Autor

Por medio del presente documento certifico que he leído todas las Políticas y Manuales de la Universidad San Francisco de Quito USFQ, incluyendo la Política de Propiedad Intelectual USFQ, y estoy de acuerdo con su contenido, por lo que los derechos de propiedad intelectual del presente trabajo quedan sujetos a lo dispuesto en esas Políticas.

Asimismo, autorizo a la USFQ para que realice la digitalización y publicación de este trabajo en el repositorio virtual, de conformidad a lo dispuesto en la Ley Orgánica de Educación Superior del Ecuador.

Nombres y apellidos: María José Villamarín Urquizo

Código: 00200299

Cédula de Identidad: 0605188861

Lugar y fecha: Quito, 14 de Mayo de 2023

ACLARACIÓN PARA LA PUBLICACIÓN

Nota: El presente trabajo, en su totalidad o cualquiera de sus partes, no debe ser considerado como una publicación, incluso a pesar de estar disponible sin restricciones a través de un repositorio institucional. Esta declaración se alinea con las prácticas y recomendaciones presentadas por el Committee on Publication Ethics COPE descritas por Barbour et al. (2017) Discussion document on best practice for issues around theses publishing, disponible en `http://bit.ly/COPETheses`

UNPUBLISHED DOCUMENT

Note: The following capstone project is available through Universidad San Francisco de Quito USFQ institutional repository. Nonetheless, this project – in whole or in part – should not be considered a publication. This statement follows the recommendations presented by the Committee on Publication Ethics COPE described by Barbour et al. (2017) Discussion document on best practice for issues around theses publishing available on `http://bit.ly/COPETheses`

Agradecimientos

Agradezco a mis padres por todo su apoyo incondicional. A mis tías y mi abuela por cuidarme y aconsejarme como si fuera suya. A mi hermana por entenderme y consolarme cuando nadie más podía. A todos los amigos que hice en el camino por estar a mi lado impulsándome a seguir; su compañía y motivación fue crucial en la culminación de esta etapa. Agradezco especialmente a el mejor de los amigos que he tenido, al que por mucho tiempo ha sido mi lugar seguro y mi mejor soporte. También agradezco a Melissa Infusino por ser mi tutora y por todo el apoyo que me ha brindado a lo largo de la carrera, y al departamento de Biología de la Universidad San Francisco de Quito por su colaboración en la realización de este proyecto.

En general, agradezco a todas las personas que me dieron una palabra de apoyo cuando la necesité, que es lo que me permitió llegar aquí. Quiero agradecer especialmente a mi abuelo por ponerme en este camino, por siempre confiar en mí y en mis sueños, por enseñarme que nada es imposible, por impulsarme a ser mejor cada día y por ser mi inspiración. Aunque no logró ver este trabajo, todo esto es para él.

Resumen

Los colores estructurales se dan por la interacción de la luz con las estructuras de los materiales, en un mecanismo que es puramente físico. Estos colores están muy presentes en la naturaleza, especialmente en insectos como los escarabajos. En el presente estudio se analiza el color estrcutural de un espécimen de *Canthon fulgidus* o escarabajo coprófago. Se demuestra que este insecto actúa como un polarizador circular izquierdo al analizar los parámetros de Stokes de la luz que refleja y se concluye que sus propiedades ópticas se deben a la esctructura helicoidal de quitina de su caparazón, que se asemejan a las de un cristal líquido colestérico.

Palabras clave: *Canthon fulgidus, colores estructurales, reflectancia, polarización, parámetros de Stokes, escarabajo.*

Abstract

Structural colors are the result of light's interaction with the structure of the materials, through a mechanism that is purely physical. These colors are very common in nature, specially among the scarab beetles. On this study we analyze the structural color of a *Canton fulgidus* specimen. We conclude that the insect acts as a left circular polarizer, and that the optical properties of its elytra are the result of a helical arrangement of chitin layers, similar to the structure of cholesteric liquid crystals.

Keywords: *Structural colors, reflectance, polarization, Stokes parameters, scarab beetle.*

Contents

List of Tables

List of Figures

Chapter 1

Introduction

1.1 Structural colors

We call structural colors to coloration that does not result from pigments on the materials, but rather from the interaction of incident light with its physical structure. [4]

The study of structural color goes back almost 400 years. In 1665, Robert Hooke analyzed the structure of the silverfish and its relation to its color. In 1730, Newton managed to describe the mechanism for coloration of peacock feathers, and after him, many scientists such as Young, Michelson and Rayleigh used their master of optics to deepen the knowledge of structural coloration. [5] [6]

However, it wasn't until 1942 with the invention of the electronic microscope that the study of structural colors began as we know it today, as electronic images offered a clear and detailed picture of the nano structures for the first time in

history. [4]

The study of structural color has been mainly focused on the iridescence of butterflies wings, as these results have been important to industrial biomimicry. Still, there is another great group in nature that displays an equally interesting array of optical structures: the insects of the order Coleoptera [5]. This beetles correspond to almost 40% of all described insects, with over 400.000 known species. Their major feature is a hard case that protects their wings called elytra. This structure is what interests us for it is what gives them their iridescence.

Iridescence consists in the change of the hue of an object that results from the variation of the angle of vision. The three main iridescent mechanisms in Coleoptera are multilayer reflectors, three-dimensional photonic crystals and diffraction gratings. [5]

Multilayer reflectors are the most common mechanism of structural colors in Coleoptera. The beetles' elytra is made of alternating thin layers of materials with low and high refraction index. When the space between the layers approaches one quarter of the visible light wavelength, constructive interference produces color. Photonic crystals mechanisms show gem-like reflectance and colors, produced by an ordered lattice of nanoscale spheres found on the elytra structure. Diffraction gratings consist of a nanoscale array of parallel slits that display a full rainbow-like color, in other words, it diffracts white light into full spectra. [4] [6]

Figure 1.1: *Canthon fulgidus* specimen[1]

1.1.1 Canthon fulgidus

The *Canthon fulgidus* is a scarab beetle found in the occidental hemisphere, specially in the tropical and subtropical areas of countries like Ecuador, Colombia, Peru and Brazil. Their average length and width are 17 mm and 8 mm respectively. They belong to the class Insecta, the order Coleoptera and the family Scarabaeidae. They exhibit a green metallic color to plain sight as shown in Figure 1.1. [7] These beetles present a structural color result of their multilayer elytra, so we will go deeper in this mechanism to study why these insects have such coloration.

1.1.2 Multilayer reflectors

Multilayer reflectors can be understood in terms of a pair of layers that appear periodically on a structure. [4] This kind of array is also known as a Bragg mirror. This mechanism is widely spread in nature, and can be as complex as the one found
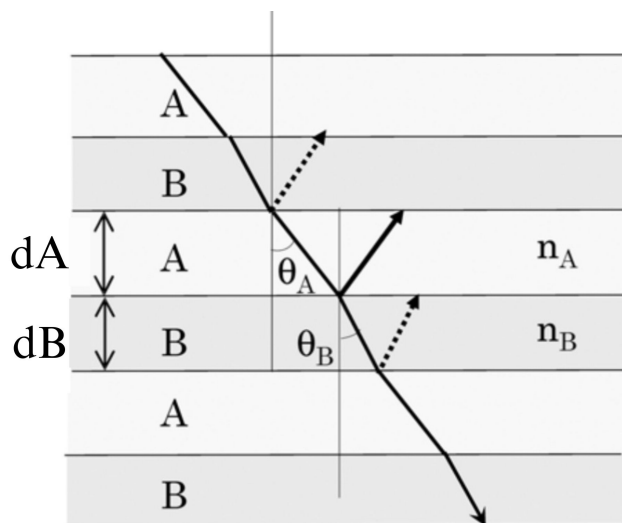
Figure 1.2: Schematic of a multilayer reflector [2]

on the beetle *Chrysina resplendens*, that posses 120 layers on its elytra, producing a metallic gold color. [8] Lets consider two layers A and B, with thickness and refractive indices d_A, d_B and n_A and n_B respectively, according to figure 1.2. Assuming $n_A > n_B$, the condition for constructive interference is

$$2(n_A d_A \cos \theta_A + n_B d_B \cos \theta_B) = m\lambda \tag{1.1}$$

Where θ corresponds to the incidence angle. Equation (1.1) can be expressed as

$$2n_j d_j = m\lambda \tag{1.2}$$

for an array with several layers, where j stands for the respective layer. If there is a difference of $\lambda(m' + \frac{1}{2})$ on the optical path for constructive interference, then equation (1.2) turns into

$$\lambda(m' + \frac{1}{2}) = 2n_j d_j \tag{1.3}$$

With m' being a positive integer number. When light comes in a normal angle, and for $m' = 0$, then from equation 1.3 we derive that $\frac{\lambda}{4} = n_j d_j$. From this result we conclude that when the layer thickness is approximately one quarter of the wavelength of the incident beam, we describe it as an ideal multi-layer reflector. When the spacing between the layers approaches one quarter wavelength of the visible light, one or more bright colors will appear given the constructive interference. On the other hand, if the stack does not fulfill this condition (i.e. the periodicity of the layers is broken or the nd is different for each layer) then we call the structure a non-ideal multilayer reflector, and it produces more dull and opaque colors [8]. Layers with greater optical thickness reflect larger wavelengths. If the thickness varies between different regions of the elytra, multiple colors may be reflected. [5] The maximun reflectance of an ideal multilayer stack is given by

$$|R|^2 = \left(\frac{1 - \left(\frac{n_A}{n_B} \right)^{2l}}{1 + \left(\frac{n_A}{n_B} \right)^{2l}} \right)^2 \tag{1.4}$$

where l is the number of pair of layers in the system. [9]

Green iridescence in scarab beetles can have different biological functions: it can be an anti-predator mechanism, that allow the beetle to disappear in the natural background. Also, since a bright green color if often associated to poisonous specimen in other species, predators may be discouraged to attack a green beetle; it is thought to be a thermo-regulation mechanism as well, by reflecting solar light the beetles can avoid over-heating and dehydration; it is also related to the social signaling among individuals of the same species, especially in mate selection [10], [5]. Studying the color mechanism in beetles such as the *Canthon fulgidus* can

help to shed some light on the insect structure, evolution and biological functions.

The Bragg reflection in *Canthon fulgidus* is made more interesting by its chiral structure. The optical behavior in this case is equivalent to the one of cholesteric liquid crystals (CLC) that have been extensively studied due to their interest as optical materials. In CLC birefringent nematic layers are arranged to form a helical structure whose pitch is comparable to the wavelength of visible light. From a structural point of view *Canthon fulgidus* is a solid equivalent of CLC, where the layers of chitin, a polysaccharide related to cellulose, are arranged helically in space. Chitin and nematic layers are both birefringent and show an equivalent optical behavior. We can therefore say that *C. fulgidus* has a cholesteric structure as well. The refractive indices of chitin can vary depending on many factors, but in beetles the average refractive index range between 1.54 and 1.56. [11].

Reflection from the cholesteric structures is complicated in comparison with simple multilayer structures such as the one showed in figure 1.2. The helical planes of CLC diffract light selectively, according to Bragg condition modified by Snell's Law [11]

$$\lambda = nP \left(1 - \frac{cos^2\theta}{n^2} \right)^{1/2} \tag{1.5}$$

where λ is the reflected wavelength, n is the mean refractive index, P is the pitch and θ is the angle of the incident light.

The expression

$$\Delta\lambda = P\Delta n \tag{1.6}$$

describes the spectral width of the selective reflection band, where $\Delta n = n_e - n_o$

is the birefringence of a layer perpendicular to the layer axis.

Reflection from the cholesteric structures is complicated in comparison with simple multilayer structures such as the one showed in figure 1.2. At the wavelength in question, light is divided into right and left circularly polarized components, and only the component of light with the same sense of rotation of electric field vectors as the helical sense of the molecular ordering is transmitted while the other handiness is reflected.

Birefringent materials such as nematic liquid crystals or chitin have a refractive index that depends on propagation direction and incident polarization. They can be bi-axial or uni-axial, showing one or two possible optical axes. According to its crystalline structure, chitin is expected to be a bi-axial material, however when chitin nanocrystals are organized in layers they show a uni-axial behavior. [12] In this section we describe briefly uni-axial materials. Birefringent optical materials can be described by means of a mathematical construction called index ellipsoid, that for a uni-axial material has cylindrical symmetry and its shown in figure 1.3.

The ellipsoid is characterized by the value n_e and n_o, that are the refractive index value in the axial direction and the radial direction respectively (optical axes is along the axial direction). The plane perpendicular to the direction of propagation of light intercepts an ellipse (dotted surface in the graph) on the ellipsoid. The ellipse main axes direction represents the electric field eigenvectors and the their lengths represent the two refractive indexes experienced. The refractive indexes values are given by

$$n = n_e(\theta) \frac{n_0 n_e}{\sqrt{n_0^2 sin^2\theta + n_e^2 cos^2\theta}} \tag{1.7}$$
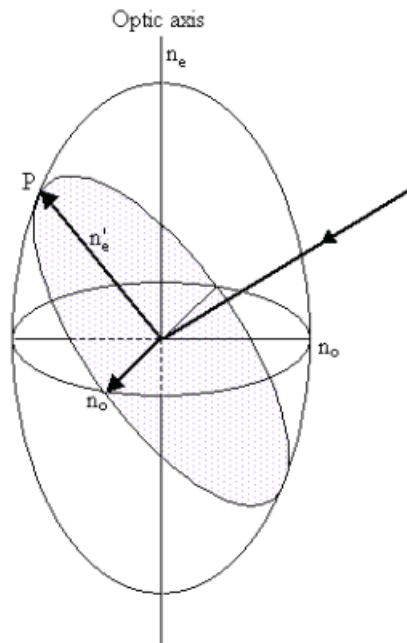
Figure 1.3: Index ellipsoid

where θ is the angle between the light wave-vector and the optical axes.

It is important mentioning that the effective refractive index depends also on the polarization of the incident field. Same direction of propagation, but different polarization correspond indeed to a different value of the effective refractive index.

1.2 Polarization

We know that light corresponds to an electromagnetic wave or, in other words, an oscillation of the electric and magnetic fields. When we talk about polarization of light, we refer to the direction of vibration of the electric field. Linear polariza-
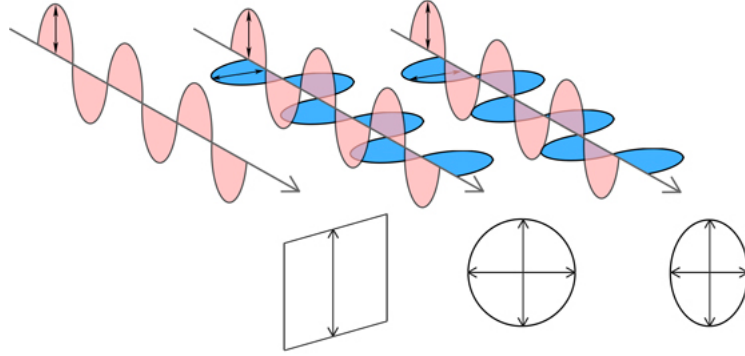
Figure 1.4: Different types of polarization: linear, circular and elliptical.

tion occurs when the electric field oscillates in a plane. In circular polarization, the electric vector draws a helix, while elliptical polarization describes any state between linear and circularly polarized light. [13] Let a plane wave be propagating along the z-direction with the following components [3]

$$E_x = E_{0x}e^{i(k_x z - \omega t)} \tag{1.8}$$

$$E_y = E_{0y}e^{i(k_y z - \omega t)} \tag{1.9}$$

where it's clear that the amplitudes are complex, as they carry a phase. We can combine the both in what is called a Jones vector for the wave, which has the form

$$\mathbf{J} = \begin{pmatrix} E_x \\ E_y \end{pmatrix} = \begin{pmatrix} E_{0x}e^{i\delta_x} \\ E_{0y}e^{i\delta_y} \end{pmatrix} \tag{1.10}$$

The electric field oscillates on the x-y plane following a trajectory that depends on the amplitude of both components and the relative phase difference between the x and y components, not on the absolute phase. This trajectory can be linear if E_x or E_y are 0, circular if $E_0 = E_y$ and the phase difference is 90, or anything in

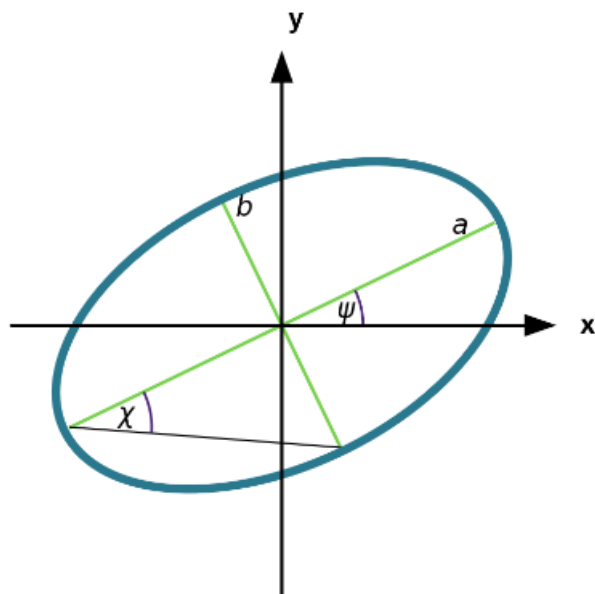between which describes an elliptical polarization. [3]

Figure 1.5: Polarization ellipse [3]

Figure 1.5 represents the polarization ellipse. The angle ψ describes the rotation of the ellipse with respect to the x-axis. The angle χ describes the ellipticity, the ratio between the length of the minor and major axis. [3] [14] The radii a and b are

$$a \;=\; E_{0x}^2 cos\psi + E_{0y}^2 sin\psi + 2E_{0x}^2 E_{0y}^2 cos\psi sin\psi cos(\delta_y - \delta_x) \qquad (1.11)$$

$$b \;=\; E_{0x}^2 sin\psi + E_{0y}^2 cos\psi + 2E_{0x}^2 E_{0y}^2 cos\psi sin\psi cos(\delta_y - \delta_x) \qquad (1.12)$$

where

$$tan2\psi = \frac{2E_{0x}E_{0y}}{E_{0x}^2 - E_{0y}^2} cos(\delta_y - \delta_x) \qquad (1.13)$$

And

$$tan\chi = \frac{b}{a} \qquad (1.14)$$

1.2.1 The Stokes parameters

The Stokes Parameters are a set of values which completely characterize the polarized state of light in terms of its intensity. Let's consider an optical beam with two orthogonal components that is propagating along the z-axis

$$E_x(z,t) = E_{0x}cos(\tau + \delta_x) \tag{1.15}$$

$$E_y(z,t) = E_{0y}cos(\tau + \delta_y) \tag{1.16}$$

Where t represents time, E_{0x} and E_{0y} the amplitudes of the field, and δ_x and δ_y phase constants. The quantity $\tau = \omega t - \kappa z$ is called the propagator and it describes the propagation of the wave. Working with equations (1.15) and (1.16) experimentally is not possible as the frequency of oscillation of light waves ω is around the order of 10^{-15} s. [14]Given that, we need to find equations that rely only on measurable parameters, i.e. the intensity.

We can rewrite equations (1.15) and (1.16) as

$$\frac{E_x(z,t)}{E_{0,x}} = cos\tau cos\delta_x - sin\tau sin\delta_x \tag{1.17}$$

$$\frac{E_y(z,t)}{E_{0,y}} = cos\tau cos\delta_y - sin\tau sin\delta_y \tag{1.18}$$

From where we obtain the following relations

$$\frac{E_x}{E_{0x}}sin\delta_y - \frac{E_y}{E_0 y}sin\delta_x = cos\tau sin(\delta_y - \delta_x) \tag{1.19}$$

$$\frac{E_x}{E_{0x}}cos\delta_y - \frac{E_y}{E_0 y}cos\delta_x = sin\tau sin(\delta_y - \delta_x) \tag{1.20}$$

Squaring and adding equations (1.19) and (1.20) yields to

$$\frac{E_x(z,t)^2}{E_{0x}^2} + \frac{E_y(z,t)^2}{E_{0y}^2} - \frac{2E_x(z,t)E_y(z,t)}{E_{0x}E_{0y}}cos\delta = sin^2\delta \tag{1.21}$$

With $\delta = \delta_y - \delta_x$. This equation is known as the polarization ellipse. We now take the time average of equation (1.21) to finally obtain observable parameters. This average is defined by

$$\langle E_i(z,t)E_j(z,t)\rangle = \lim_{T\to\infty}\frac{1}{T}\int_0^T E_i(z,t)E_j(z,t)dt \tag{1.22}$$

With $i,j = x,y$. Using equation 1.22 with equation 1.21 and operating, we finally obtain the relation

$$S_0^2 = S_1^2 + S_2^2 + S_3^2 \tag{1.23}$$

where

$$S_0 = E_{0x}^2 + E_{0y}^2 \tag{1.24}$$

$$S_1 = E_{0x}^2 - E_{0y}^2 \tag{1.25}$$

$$S_2 = 2E_{0x}E_{0y}cos\delta \tag{1.26}$$

$$S_3 = 2E_{0x}E_{0y}sin\delta \tag{1.27}$$

Equations (1.24) to (1.27) are the four Stokes parameters. As they are in terms of intensities (amplitude squared) they are measurable. S_0 corresponds to the total intensity, S_1 to the linear horizontal polarization, S_2 to the linear 45° polarization and S_3 to the right circular polarization. The Stokes parameters are usually placed in form of a column vector and normalized to S_0. Table 1.1 explains the meaning of

the values of the Stokes parameters.[14], while table 1.2 shows the stokes vector's components for some common forms of polarization.

$$\mathbf{S} = \frac{1}{S_0} \begin{pmatrix} 1 \\ S_1 \\ S_2 \\ S_3 \end{pmatrix}$$

Table 1.1: Interpretation of the normalized stokes parameters

Stokes parameter	Meaning	Posible values
S_0	Total intensity	1
S_1	Horizontal vs. Vertical	$1 \geq S_1 \geq -1$
S_2	45 vs. -45	$1 \geq S_2 \geq -1$
S_3	Right vs. Left handedness	$1 \geq S_3 \geq -1$

Table 1.2: Stokes vector components for different normalized polarizations

LHP	LVP	L+45	L-45	RCP	LCP
1	1	1	1	1	1
1	-1	0	0	0	0
0	0	1	-1	0	0
0	0	0	0	1	-1

Equation (1.23) works only when light is completely polarized. For partially polarized light, this equation transforms into

$$S_0^2 > S_1^2 + S_2^2 + S_3^2 \tag{1.28}$$

Partially polarized light can be described as a combination of polarized light and

unpolarized light. The degree of polarization P can be computed as

$$P = \frac{\sqrt{S1^2 + S_2^2 + S_3^2}}{S_0} \tag{1.29}$$

Clearly, $0 \geq P \geq 1$. [14]

It is possible to put the Stokes vectors on a graphical representation. For this, the Poincare sphere, shown in figure 1.6 is used.
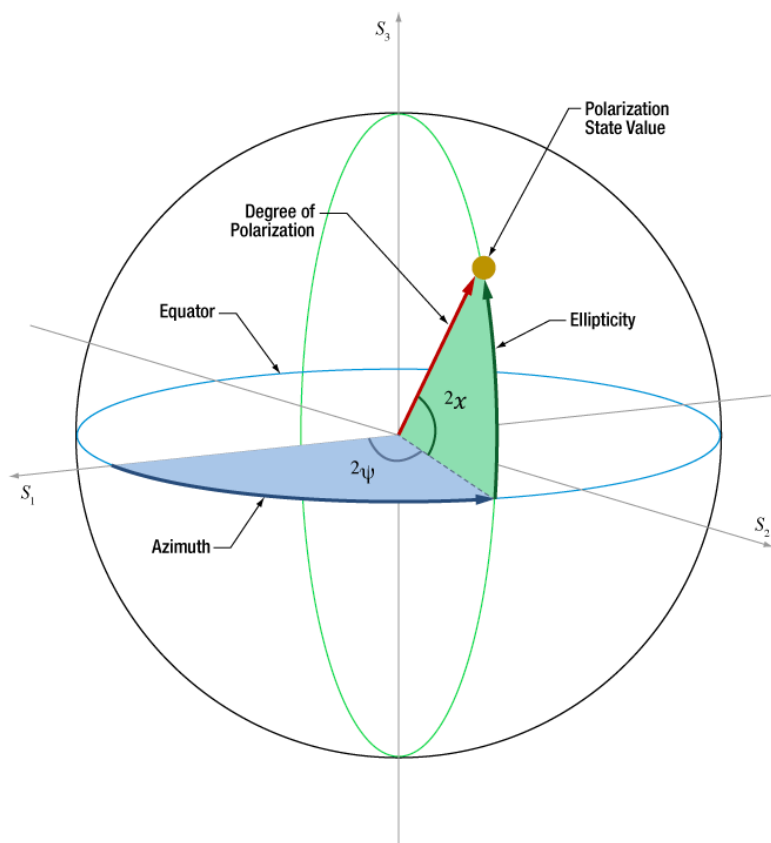

Figure 1.6: Poincare Sphere [3]

Polarization states are placed into the Poincare sphere using a coordinate system like the one of latitude and longitude used to locate points on the Earth's globe. The place of the points in the sphere are determined using two angular values and a radius. The angular values are the same as the ones found for the polarization ellipse (equations 1.13 and 1.14). The radius depends on the degree of polarization. For fully polarized light, it's value is equal to one and the point is located over the sphere; for partially polarized light the value P acts as the radius, and the point would be inside the sphere. The equivalence between the Stokes vector and the angles of the polarization ellipse are [3] [14]

$$
\mathbf{S} = \begin{pmatrix} S_0 \\ S_1 \\ S_2 \\ S_3 \end{pmatrix} = \begin{pmatrix} S_0 \\ cos2\psi cos2\chi \\ sin2\psi cos2\chi \\ sin2\chi \end{pmatrix}
\tag{1.30}
$$

The goal of this work is to describe the structural color of a C. fulgidus specimen by obtaining and analyzing the Stokes parameters of the reflected light produced by the elytra. The information obtained from the measurable optical properties will be used to describe the structure as accurately as possible. Such information can be potentially used to improve the understanding of the relation between structures and their corresponding optical properties, which is of interest for the area of biomimetics, and can work as inspiration for bioreflectors, coatings, polarization filters, sensor devices, etc.

Chapter 2

Methods

2.1 Reflectance Analysis

Before all measurements, the elytras over both wings of the beetle were removed carefully using tweezers. Once they were ready, they were secured over microscope slides with 5 mm transparent double sided tape.

For the reflectance measurements, the components used were: a FLAME-S-VIS-NIR spectrometer, a Tungsten Halogen Light Source, a reflection probe, a probe holder and a reflection standard. All components came from the company Ocean Optics. The first step into measurement of the reflectance spectra is to calibrate the OceanView software. In order to do this, we need to set the reference spectrum for light and dark measurements. The experimental set-up for this is shown in figure 2.1.
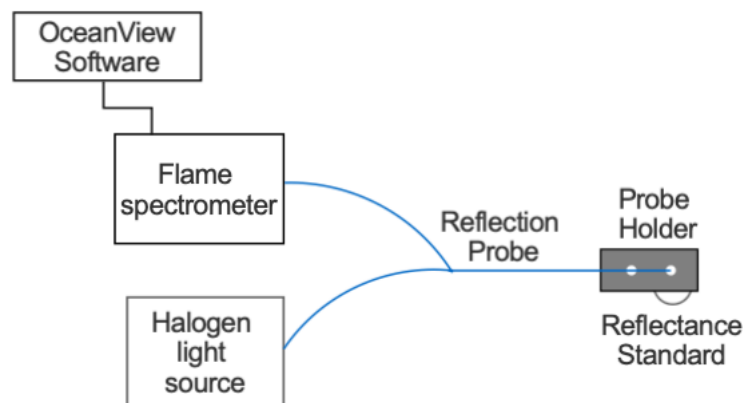
Figure 2.1: Experimental set up for reflectance measurement

Once the software was calibrated, the reflectance standard in figure 2.1 was replaced by the elytra sample. Then the measurement was performed at normal incidence. The obtained reflectance spectrum will be also useful at the moment we need to describe the structure of the beetle.

2.2 Experimental determination of the Stokes parameters

2.2.1 Classic case

The classic case of the measurement of the Stokes parameters uses two polarizing elements called a retarder and a polarizer. On this case, we use a quarter waveplate and a linear polarizer. A monochromatic incident beam after going through both
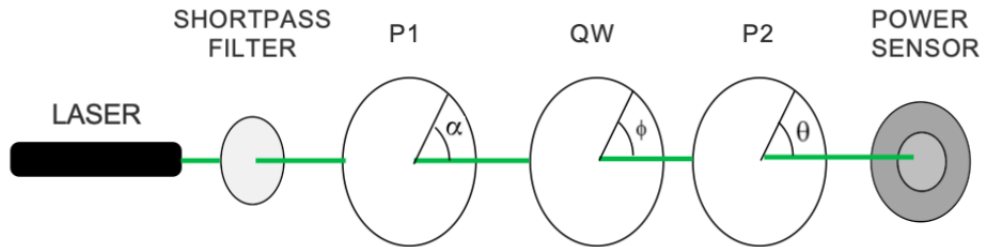
Figure 2.2: Experimental set-up for the measurement of the laser Stokes Parameters. Note that the angles are measured with respect to the horizontal.
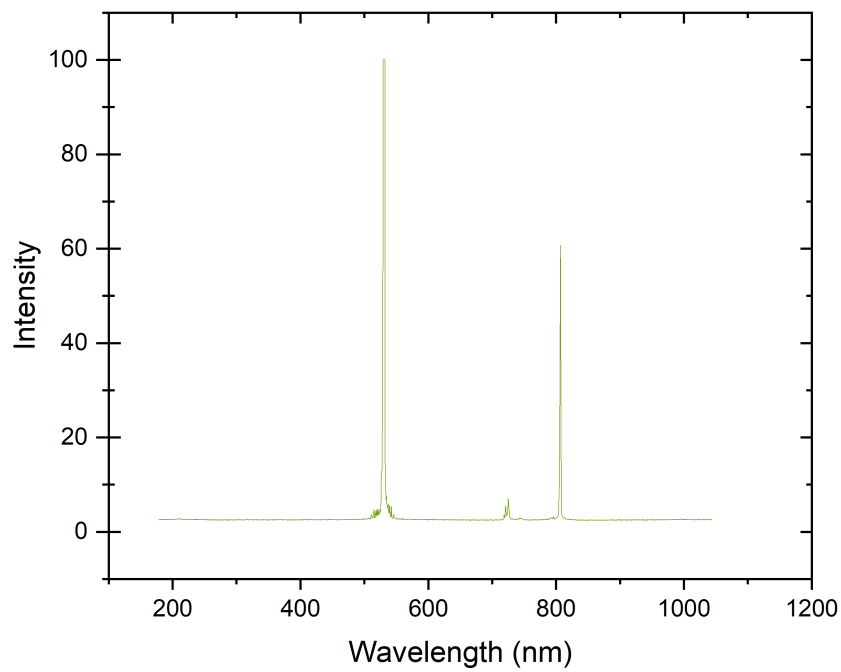

Figure 2.3: Laser analysis

of these components has an intensity [15]

$$I(\theta,\phi) = \frac{1}{2}\left[S_0 + S_1 cos2\theta + S_2 cos\phi sin2\theta + S_3 sin\phi sin2\theta\right] \qquad (2.1)$$

Where θ corresponds to the angle of the polarizer and ϕ to the waveplate. The first three Stokes parameters are measured without the retarder, which we denote with $\phi = \mathbf{0}$, and by measuring the light intensity at θ =0°,90°,45°,-45°. Then, we reinsert the retarder in an angle of $\phi = 0°$ (parallel to the table) to take two more measures with θ =45°,-45°. In total, we take six measures of intensity. Then, the stokes parameters can be computed from the intensities as follows [15]

$$S_0 = I(0,\mathbf{0}) + I(90,\mathbf{0}) \qquad (2.2)$$

$$S_1 = I(0,\mathbf{0}) - I(90,\mathbf{0}) \qquad (2.3)$$

$$S_2 = I(45,\mathbf{0}) - I(-45,\mathbf{0}) \qquad (2.4)$$

$$S_3 = I(45,0) - I(-45,0) \qquad (2.5)$$

For this study, we computed the Stokes parameters for the incident beam (laser alone) and the reflected beam from the sample. The measurements were taken with a polarized incident beam of linear horizontal, vertical, 45° and -45° polarization. To control the polarization of the incident beam a polarizer P1 was placed next to the laser. The experimental set ups for the measurement of the Stokes parameters are shown in figures 2.2 and 2.4.These set ups contain a short pass filter with cut-off wavelength of 700 nm, as the laser that was used had a component on the infrared (aprox. 800 nm) as shown in figure 2.3. This component was removed for the experiment as it was affecting the stability of the measurements.
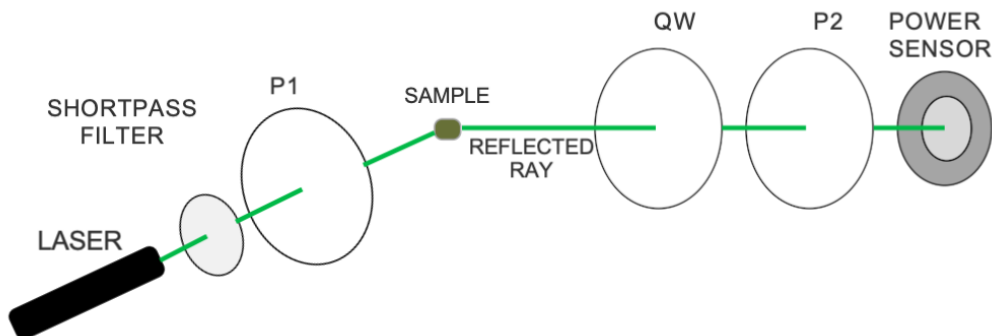
Figure 2.4: Experimental set-up for the measurement of the Stokes parameters of the reflected beam

2.2.2 Phase difference error case

While polarizers can be designed to be used over a range of wavelengths, waveplate retarders are wavelength specific and need to be used with a matching laser. However, the retarder can still be used to measure the Stokes parameters if a correction is done on the parameter S_3. To compute this correction we use the formula [15]

$$S_{3c} = \frac{I(\theta, \phi) - I(\theta, \phi + 90)}{cos(\Delta\rho)sin2(\phi - \theta)} \tag{2.6}$$

With [16]

$$\Delta\rho = \frac{\pi}{2}\left(1 - \frac{\lambda_{wp}}{\lambda_i}\right) \tag{2.7}$$

where λ_{wp} is the retarder designed wavelength and λ_i is the wavelength of the incident light.

Chapter 3
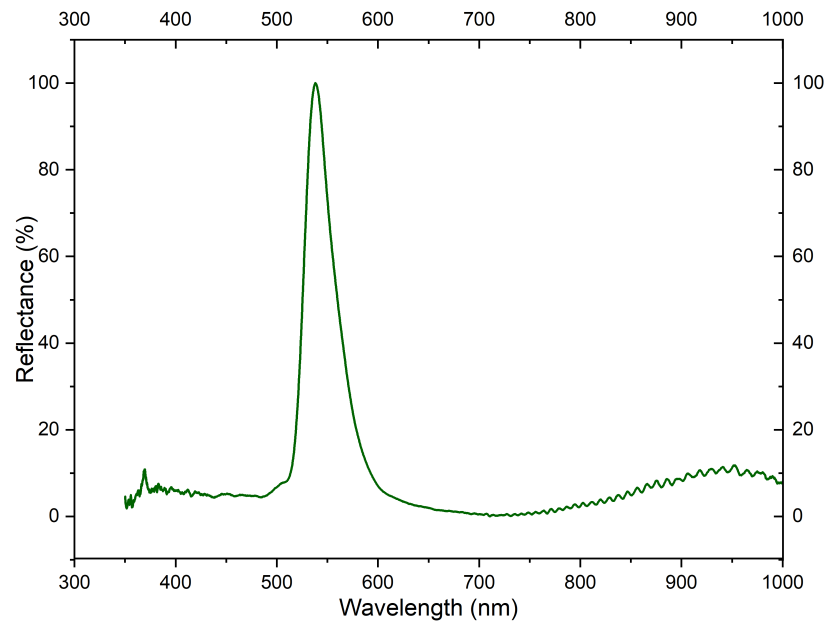
Results

3.1 Reflectance analysis

Figure 3.1: Reflectance obtained at normal incidence

The resulting curve from the reflectance measurement of the sample is shown on figure 3.1. It shows a clear peak at green as expected from the beetles color. The sources available at the laboratory had a wavelength of 532 nm, 633 nm and 780 nm. From figure 3.1 we see that both 633 nm and 780 nm produced a reflection of less of 10%, so the laser chosen to do the Stokes analysis was the 532 nm, which produces a reflection of approximately 85%.

Also from figure 3.1, we can see that the maximum reflectance is obtained at 537.956 nm. The average index of refraction of chitin is 1.54. Putting this information on equation (1.5), and considering the reflection at normal incidence, we obtain a pitch value of $P = 349.32$ nm.

A Gaussian fit was applied to the reflectance curve, where we obtained a FWHM value of 35.51 nm. Using this value as $\Delta\lambda$, and with the previous computed value of P, we can find the birefringence value with equation (1.6). The result is $\Delta n = 0.1$, which matches the studies that place chitin refraction index between 1.5 and 1.6 [12] [17].

If, in equation (1.4), we place $n_A = 1.6$ and $n_B = 1.5$, and take the maximum reflection of 0.89 obtained with the Gaussian fit we can solve for l, obtaining a total of 21 layers on the structure.

Table 3.1: Obtained Stokes parameters. This table contains the corrected S3 value for the reflected and incident beams on the four different polarizations studied.

	Vertical		Horizontal		45		-45	
	I	**R**	**I**	**R**	**I**	**R**	**I**	**R**
S0	1,00	1,00	1,00	1,00	1,00	1,00	1,00	1,00
S1	-0,81	-0,44	0,64	0,12	0,06	-0,18	-0,05	-0,20
S2	0,06	0,26	-0,04	0,20	0,62	0,40	-0,82	-0,05
S3	0,01	-0,48	-0,01	-0,59	0,00	-0,57	0,00	-0,52

3.2 Polarization

The experiment was conducted using a 532 nm laser with a quarter waveplate designed for a 633 nm laser, so it was necessary to compute a corrected S_3. The measurements taken to use with equation (2.6) were $I(0, -45)$ and $I(0, 45)$ as suggested by Kihara [15], and the resulting value of $\Delta\rho$ was $0,300$. The analysis of the Stokes Vectors of light before and after being reflected by the beetle shows a strong shift to left circular polarization. Parameter S_3, which takes values from -1 for completely left circular polarization to 1 for complete right circular polarization, decreases for all forms of incident light, approaching the negative one. In figure 3.2 we see the polarization ellipse for incident and reflected light which transforms from linear to elliptical. Table 3.1 shows the obtained normalized Stokes parameters for the incident beam (laser only) and the reflected beam, while table 3.3 shows the difference between the S_3 parameter obtained with the classic method vs. the corrected method.

The beetle does not act as a perfect polarizer, as we can see from the degree of polarization of the reflected beam, shown on table 3.2, and the fact that the resulting states are not perfectly circular.

Table 3.2: Degree of polarization of the reflected beam

Incident beam polarization	Resulting degree of polarization
Vertical	0,49
Horizontal	0,40
45	0,51
-45	0,31

Table 3.3: Comparison between the S_3 obtained with the classical method and the one obtained with the phase difference method

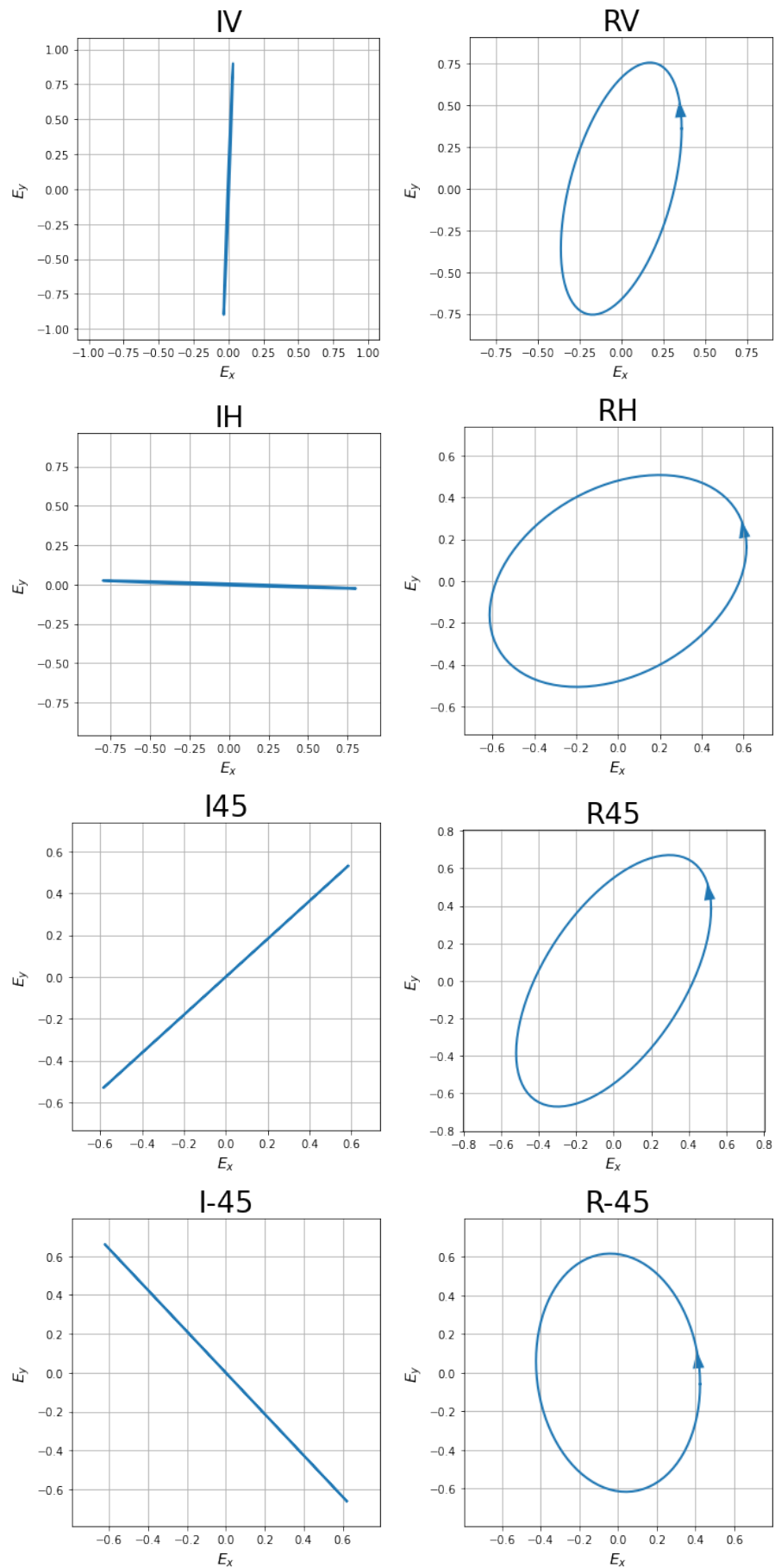| Polarization		S_3	Corrected S_3
Vertical	Incident	0,35	0,01
	Reflected	-0,58	-0,48
Horizontal	Incident	0,02	-0,01
	Reflected	-0,66	-0,59
45	Incident	0,25	0,00
	Reflected	-0,71	-0,57
-45	Incident	0,33	0,00
	Reflected	-0,47	-0,52

Figure 3.2: Polarization ellipses

Chapter 4

Conclusions

The *Canthon fulgidus* presents a multilayer elytra formed by layers of birefrigent chitin that are stacked helically with a left handedness, similar to the structure shown on figure 4.1.

On this work, we have been able to explain with detail the phenomenology of the mechanism that gives the *C. fulgidus* its color. Every polarization can be
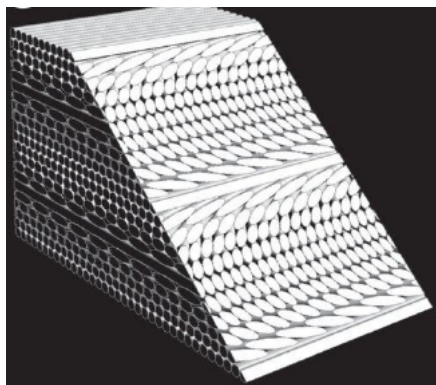

Figure 4.1: Helical multilayer structure similar to that of the *Canthon fulgidus*
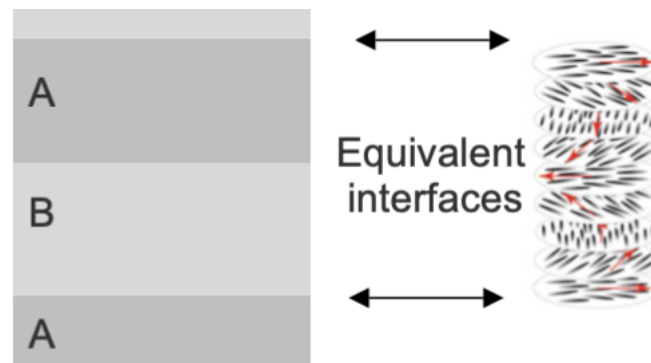
Figure 4.2: Equivalence between multilayer structures

decomposed in terms of two perpendicular polarizations with different handiness. When light shines the beetles helical structure, the effective refractive index will be determined by reciprocal orientation of the optical electric field and the index ellipsoid. If the circular polarization has the same handiness of the chiral structure and the pitch is comparable with the wavelength (within the space of a wavelength the optical field completes an entire turn), the optical field maintain the same orientation with respect to the following ellipsoid of index: the effective refractive index is the same for the all way. As a consequence light is transmitted without any disturbance as in an homogeneous medium. The other polarization is able to see a variation of index within the space of a pitch, thus experiencing Bragg reflection. The pitch is the distance that must be traveled so that the light come back to the same effective refractive index.

Even thought the *Canthon fulgidus* presents a more complex mechanism to simple multilayer reflectors, the general principle holds, as the helical multilayer is equivalent, as shown in figure 4.2. The constructive interference that occurs with every reflected ray of the structure results in a 537 nm ray, that appears as a shiny green to sight.

These results are in good accordance to previous research on structural color, because even when there is no extensive research on *Canthon fulgidus*, there are studies that analyze the structural color of beetles with similar characteristics. The result support the claim that the insects of the family Scarabidae with green metallic coloration act as a polarizer, as we found out from the Stokes analysis of the reflected beam.

We were also able to obtain a good guess of the structure of the beetle from the results of optical measurements, finding a birefringence of 1.5-1.6, a pitch of 349.32 nm and 21 layers in the structure.

Given that we obtained a good result even with non-ideal materials (unstable laser pointer and not wavelength matching quarter waveplate), this study shows that similar experiments can be done on didactic environments, as it is not necessary to have extremely precise equipment to observe the physical effects.

Bibliography

[1] Redtenbacher. Canthon fulgidus.

[2] S. Kinoshita, S. Yoshioka, and J. Miyazaki. Physics of structural colors. *Reports on Progress in Physics*, 71(7):076401, Jun 2008.

[3] M. Baier. *Polarization multiplexed photonic integrated circuits for 100 Gbit/s and beyond.* PhD thesis, Aug 2018.

[4] Andrew Richard Parker. 515 million years of structural colour. *Journal of Optics A: Pure and Applied Optics*, 2(6):R15, Nov 2000.

[5] Ainsley E Seago, Parrish Brady, Jean-Pol Vigneron, and Tom D Schultz. Gold bugs and beyond: a review of iridescence and structural colour mechanisms in beetles (coleoptera). *Journal of The Royal Society Interface*, 6(suppl$_2$) : $S165-S184, Oct 2008.$

[6] Andrew R. Parker and Natalia Martini. Structural colour in animals—simple to complex optics. *Optics Laser Technology*, 38(4):315–322, Jun 2006.

[7] Luis Gabriel de O. A. Nunes, Rafael V. Nunes, and Fernando Z. Vaz-de Mello. Taxonomic revision of the south american subgenus canthon (goniocanthon) pereira

martínez, 1956 (coleoptera: Scarabaeidae: Scarabaeinae: Deltochilini). *European Journal of Taxonomy*, (437437), May 2018.

[8] Jiyu Sun, Bharat Bhushan, and Jin Tong. Structural coloration in nature. *RSC Advances*, 3(35):14862–14889, Aug 2013.

[9] M. F. Land. The physics and biology of animal reflectors. *Progress in Biophysics and Molecular Biology*, 24:75–106, Jan 1972.

[10] Kevina Vulinec. Iridescent dung beetles: A different angle. *The Florida Entomologist*, 80(2):132–141, 1997.

[11] Guram Chilaya. *Cholesteric Liquid Crystals: Optics, Electro-optics, and Photo-optics*, page 159–185. Partially Ordered Systems. Springer, New York, NY, 2001.

[12] A. Mendoza-Galván, E. Muñoz-Pineda, K. Järrendahl, and H. Arwin. Birefringence of nanocrystalline chitin films studied by mueller-matrix spectroscopic ellipsometry. *Optical Materials Express*, 6(2):671–681, Feb 2016.

[13] Eugene Hecht. *Optics*. Pearson Education, Inc., 2016.

[14] Dennis H. Goldstein. *Polarized Light*. CRC Press, Dec 2017. Google-Books-ID: cAlEDwAAQBAJ.

[15] Toshiki Kihara. Stokes parameters measurement of light over a wide wavelength range by judicious choice of azimuthal settings of quarter-wave plate and linear polarizer. *Optics Communications*, 110(5):529–532, Sep 1994.

[16] Justin Peatross and Michael Ware. Physics of light and optics.

[17] E. S. Castle. The double refraction of chitin. *Journal of General Physiology*, 19(5):797–805, May 1936.